2009 International Symposium on Nonlinear Theory and its Applications
NOLTA'09, Sapporo, Japan, October 18-21, 2009

Reflection Mechanisms of a Phase-Inversion Wave at an Edge of 2D Lattice Oscillators

Hitoshi ABURATANI†, Suguru YAMANE†, Masayuki YAMAUCHI† and Yoshifumi NISHIO‡

†Department of Electronics and Computer Engineering,
Hiroshima Institute of Technology
2-1-1, Miyake, Saeki-ku, Hiroshima , Japan
‡Department of Electrical and Electronic Engineering,
Tokushima University
2-1 Minami-Josanjima, Tokushima, Japan
Email: ab.hitoshi247@gmail.com

Abstract—We investigate synchronization phenomena on coupled oscillators system that van der Pol oscillators are coupled by inductors as a lattice. In the lattice oscillators, the phase-inversion waves, which are phenomena changing phase states between adjacent oscillators from in-phase synchronous to anti-phase synchronous or from anti-phase synchronous to in-phase synchronous and exists in steady state, were discovered. This paper clarifies reflection mechanisms of a phase-inversion wave at the edge by using instantaneous frequencies of each oscillator and phase differences between adjacent oscillators in the lattice shape system.

1. Introduction

Many investigations and analyses for synchronous systems are carried out up to now[1]–[4]. A lot of kinds of synchronization phenomena exists anywhere and anytime. For example, there are synchronous between sea waves and ship motion, earthquake and buildings, and so on. Therefore, synchronization phenomena may bring on disaster. We think that these problems of the natural world may be clarified by analyzing many synchronization phenomena. Moreover, we think that the time-series data of natural world become to be able to predict by using a synchronization system. By investigating the synchronization phenomena of coupled oscillators, we believe that various synchronization phenomena can be modeled using the electrical circuits. We observe the various phenomena on coupled oscillators system, and analyze these mechanisms[5].

In our previous study, we investigated phenomena in systems that many van der Pol oscillators were coupled as a lattice shape. The coupling parameter and the nonlinearity of the system were changed, and the existing region of phase-inversion waves were made clear[6]. Moreover, we developed the prediction system of the time-series data using the lattice oscillators. The chaos time-series data of Inaba's circuit and Chua's circuit were predicted by this system[7].

In this paper, we analyzes two kinds of reflection phenomena of the phase-inversion waves using instantaneous frequencies of each oscillator and phase differences between adjacent oscillators at an edge in the lattice shape system. The mechanisms of each reflection phenomenon are made clear.

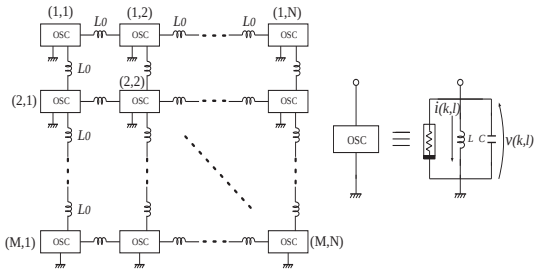

Figure 1: Circuit Model.

2. Circuit model

A lot of van der Pol oscillators are coupled by inductors L_0 as a lattice(see Fig. 1). The number of column of the system is assumed as M. The number of row of the system is assumed as N. The name of each oscillator are assumed to be OSC(k,l). A voltage of each oscillator is named $v_{(k,l)}$, and a current of inductor of each oscillator is named $i_{(k,l)}$(see Fig. 1). The circuit equations of the circuit model are normalized by Eq. (1), and the normalized circuit equations are shown as Eqs. (2)–(6).

$$\begin{aligned} &i_{(k,l)} = \sqrt{\frac{Cg_1}{3Lg_3}}x_{(k,l)}, \quad v_{(k,l)} = \sqrt{\frac{g_1}{3g_3}}y_{(k,l)}, \\ &t = \sqrt{LC}\tau, \quad \frac{d}{d\tau} = \text{“ } \cdot \text{ ”}, \alpha = \frac{L}{L_0}, \quad \varepsilon = g_1\sqrt{\frac{L}{C}}. \end{aligned} \tag{1}$$

[Corner–top (left and right)]

$$\begin{aligned} &\frac{dx_{(1,a)}}{d\tau} = y_{(1,a)}, \\ &\frac{dy_{(1,a)}}{d\tau} = -x_{(1,a)} + \alpha(x_{(1,b)} + x_{(2,a)} - 2x_{(1,a)}) \\ &\qquad\qquad + \varepsilon(y_{(1,a)} - \frac{1}{3}y_{(1,a)}^3), \end{aligned} \tag{2}$$

left:$a = 1$ and $b = 2$. right:$a = N$ and $b = N - 1$.

[Corner–bottom (left and right)]

$$\frac{dx_{(M,a)}}{d\tau} = y_{(M,a)}, \tag{3}$$
$$\frac{dy_{(M,a)}}{d\tau} = -x_{(M,a)} + \alpha(x_{(M-1,a)} + x_{(M,b)} - 2x_{(M,a)}) + \varepsilon(y_{(M,a)} - \tfrac{1}{3}y^3_{(M,a)}),$$

left:$a = 1$ and $b = 2$. right:$a = N$ and $b = N - 1$.
[Center]

$$\frac{dx_{(k,l)}}{d\tau} = y_{(k,l)}, \tag{4}$$
$$\frac{dy_{(k,l)}}{d\tau} = -x_{(k,l)} + \alpha(x_{(k+1,l)} + x_{(k-1,l)} + x_{(k,l+1)} + x_{(k,l-1)} - 4x_{(k,l)}) + \varepsilon(y_{(k,l)} - \tfrac{1}{3}y^3_{(k,l)}),$$

$1 < k < M$. $1 < l < N$.
[Edge–top and bottom]

$$\frac{dx_{(a,l)}}{d\tau} = y_{(a,l)}, \tag{5}$$
$$\frac{dy_{(a,l)}}{d\tau} = -x_{(a,l)} + \alpha(x_{(a,l-1)} + x_{(a,l+1)} + x_{(b,l)} - 3x_{(a,l)}) + \varepsilon(y_{(a,l)} - \tfrac{1}{3}y^3_{(a,l)}),$$

top:$a = 1$ and $b = 2$. bottom:$a = M$ and $b = M - 1$.
both:$1 < l < N$.
[Edge–left and right]

$$\frac{dx_{(k,a)}}{d\tau} = y_{(k,a)}, \tag{6}$$
$$\frac{dy_{(k,a)}}{d\tau} = -x_{(k,a)} + \alpha(x_{(k-1,a)} + x_{(k+1,a)} + x_{(k,b)} - 3x_{(k,a)}) + \varepsilon(y_{(k,a)} - \tfrac{1}{3}y^3_{(k,a)}),$$

left:$a = 1$ and $b = 2$. right:$a = N$ and $b = N - 1$.
both:$1 < k < M$.

The α is a coupling parameter of each oscillator. The ε is a nonlinearity of each oscillator. This system is simulated by the fourth order Runge-Kutta methods using Eqs. (2)-(6).

3. Reflection mechanisms at an edge

The phase-inversion waves shows in Fig.2. The reflection mechanisms at an edge are made clear using instantaneous frequency of each oscillator and phase difference between adjacent oscillators. The coupling parameter is fixed as $\alpha = 0.01$, and nonlinearity is fixed $\varepsilon = 0.050$. An equation of the instantaneous frequency of OSC(k, l) is calculated as follows. The instantaneous frequency is named $f_{(k,l)}(a)$ where "α" expresses the number of times of the peak value of the voltage. Time of a peak value of the voltage of OSC(k, l) is assumed as $\tau_{(k,l)}(a)$(see Fig.3). Similarly, $\tau_{(k+1,l)}(a)$ and $\tau_{(k,l+1)}(a)$ are decided. The $f_{(k,l)}(a)$ is obtained by Eq.(7).

$$f_{(k,l)}(a) = \frac{1}{\tau_{(k,l)}(a) - \tau_{(k,l)}(a-1)}. \tag{7}$$

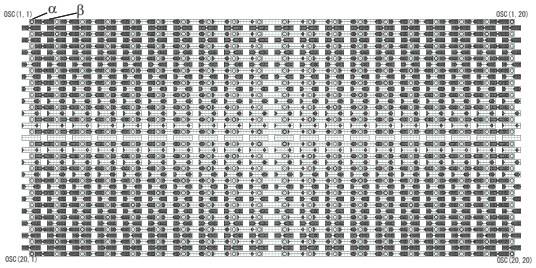

Figure 2: The phase-inversion waves on 20×20 oscillators(α:an attractor of each oscillator(current vs. voltage), β:a sum of voltages of adjacent oscillators(sum of voltage vs. time)).

Three frequencies are observed in steady states. In this system, the synchronous for vertical direction and horizontal direction needs to be considered, because this system is 2 dimensional array. Therefore, three type synchronizations are observed as follows:
1. OSC(k, l)–OSC(k, $l+1$), OSC(k, l)–OSC(k, $l-1$), OSC(k, l)–OSC($k+1$, l), and OSC(k, l)–OSC($k-1$, l): in-phase synchronous.
2. {OSC(k, l)–OSC(k, $l+1$) and OSC(k, l)–OSC(k, $l-1$): in-phase synchronous. OSC(k, l)–OSC($k+1$, l), and OSC(k, l)–OSC($k-1$, l): anti-phase synchronous.} **or** {OSC(k, l)–OSC(k, $l+1$), and OSC(k, l)–OSC(k, $l-1$): anti-phase synchronous. OSC(k, l)–OSC($k+1$, l), and OSC(k, l)–OSC($k+1$, l): in-phase synchronous.}
3. OSC(k, l)–OSC(k, $l+1$), OSC(k, l)–OSC(k, $l-1$), OSC(k, l)–OSC($k+1$, l), and OSC(k, l)–OSC($k+1$, l): anti-phase synchronous.
In this paper, we call the 1st type synchronous "in-and-in-phase synchronous." The 2nd type synchronization is called "in-and-anti-phase synchronous." The 3rd type synchronization is called "anti-and-anti-phase synchronous." An each instantaneous frequency of OSC(k, l) is obtained in each synchronous type. In the 1st situational synchronous, $f_{(k,l)}$ is f_{in-in}. In the 2nd situational synchronous, $f_{(k,l)}$ is $f_{in-anti}$. In the 3rd situational synchronous, $f_{(k,l)}$ is $f_{anti-anti}$.

The phase difference is calculated as follows. A phase difference between OSC(k, l) and OSC($k+1$, l) and a phase difference between OSC(k, l) and OSC(k, $l+1$) are calculated. The phase differences are assumed as $\Phi_{(k,l)(k+1,l)}(a)$ and $\Phi_{(k,l)(k,l+1)}(a)$ respectively.The $\Phi_{(k,l)(k+1,l)}(a)$ and $\Phi_{(k,l)(k,l+1)}(a)$ are obtained by Eq.(8).

$$\Phi_{(k,l)(k+1,l)}(a) = \frac{\tau_{(k,l)}(a) - \tau_{(k+1,l)}(a)}{\tau_{(k,l)}(a) - \tau_{(k,l)}(a-1)} \times 180 \text{ [degree]}$$
$$\Phi_{(k,l)(k,l+1)}(a) = \frac{\tau_{(k,l)}(a) - \tau_{(k,l+1)}(a)}{\tau_{(k,l)}(a) - \tau_{(k,l)}(a-1)} \times 180 \text{ [degree]}. \tag{8}$$

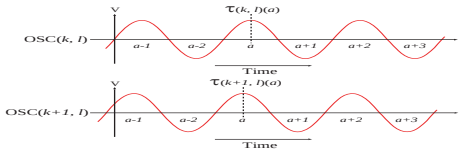

Figure 3: The detection method of frequencies and the phase differences.

Table 1: Reflection mechnism of a phase-inversion wave at an edge in in-and-anti phase synchronous(see Fig.4).

no.	*Mechanism*
0	The phase state between adjacent oscillators of the horizontal direction is the in-phase synchronous. A phase-inversion wave, which propagates from OSC(9,48) in in-phase synchronous, arrives at OSC(2,48).
1	$f_{(2,48)}$ starts to increase from f_{in-in} toward $f_{in-anti}$ by the phase-inversion wave. $f_{(2,48)}$ can not arrive at $f_{anti-anti}$ because phase states of horizontal directions of these oscillators are in-phase synchronous.
2	$\Phi_{(1,48)(2,48)}$ starts to increase toward 180 degrees from 0 because $f_{(2,48)}$ increases toward $f_{in-anti}$.
3	$f_{(1,48)}$ starts to increase from f_{in-in} toward $f_{in-anti}$ because $\Phi_{(1,48)(2,48)}$ increases toward 180 degrees.
4	$\Phi_{(0,48)(1,48)}$ starts to increase toward 180 degrees from 0, because $f_{(1,48)}$ increases toward $f_{in-anti}$.
5	$f_{(0,48)}$ starts to increase toward $f_{in-anti}$ because $\Phi_{(0,48)(1,48)}$ increases toward 180 degrees.
6	$\Phi_{(1,48)(2,48)}$ arrives around 180 degrees, and is stablilized as the anti-phase synchronous.
7	$f_{(1,48)}$ arrives around $f_{in-anti}$.
8	$f_{(1,48)}$ arrives at $f_{in-anti}$, and $\Phi_{(0,48)(1,48)}$ becomes around 180 degrees. However, in these parameters, OSC(0,48) can not stablilize for vertical direction. Therefore, $f_{(0,48)}$ becomes middle of f_{in-in} and $f_{in-anti}$, and decreases to f_{in-in} again.
9	$f_{(1,48)}$ starts to decrease from $f_{in-anti}$ toward f_{in-in} because $\Phi_{(0,48)(1,48)}$ increases toward 360 degrees.
10	$\Phi_{(1,48)(2,48)}$ starts to increase toward 360 degrees from 180 because $f_{(1,48)}$ decreases toward f_{in-in}.
11	$f_{(0,48)}$ arrives around f_{in-in}, and becomes stable.
12	$\Phi_{(0,48)(1,48)}$ arrives around 360 degrees and becomes stable.
13	$\Phi_{(0,48)(1,48)}$ arrives around 360 degrees, and $f_{(1,48)}$ arrives around f_{in-in} and becomes stable.
14	$f_{(1,48)}$ arrives around f_{in-in}, and $\Phi_{(1,48)(2,48)}$ arrives around 360 degrees and becomes stable.

The phase-inversion waves are generated by the following method. 1. Voltages and currents of all oscillators are set as same value, in other words all oscillators are set as in-phase synchronization. 2. The signs of $x_{(k,l)}$ and $y_{(k,l)}$ of arbitrary oscillators are inverted instantaneously.

3.1. Reflection of phase-inversion waves in in-and-in-phase synchronous

We can observe that a phase-inversion wave for a vertical direction in each column propagate in in-and-anti-phase synchronous. A mechanism is shown as Tab.1. A mechanism of a phase-inversion wave for a horizontal direction can be explained same method.

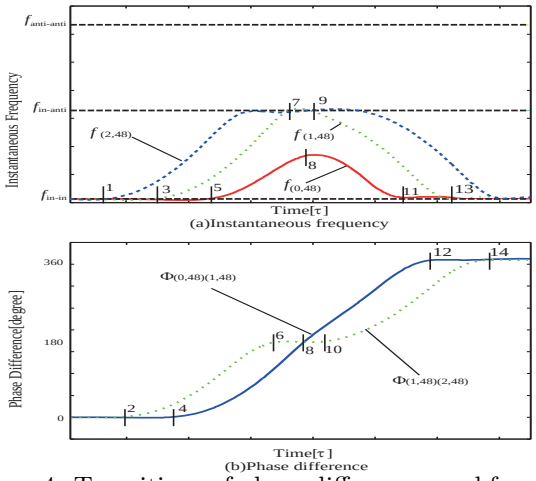

Figure 4: Transitions of phase differences and frequencies by reflecting a phase-inversion wave in in-and-in-phase synchronous.

In Fig.4(a), the vertical axis is the instantaneous frequency, and the horizontal axis is time. In Fig.4(b), the vertical axis expresses the phase difference and the horizontal axis expresses time.

3.2. Reflection of phase-inversion waves in in-and-anti-phase synchronous

We can observe that a phase-inversion wave for a vertical direction in each column propagate in in-and-anti-phase synchronous. A mechanism is shown as Tab.2. A mechanism of a phase-inversion wave for other edges can be explained same method. In Fig.5(a), the vertical axis is the instantaneous frequency, and the horizontal axis is time. In Fig.5(b), the vertical axis expresses the phase difference and the horizontal axis expresses time.

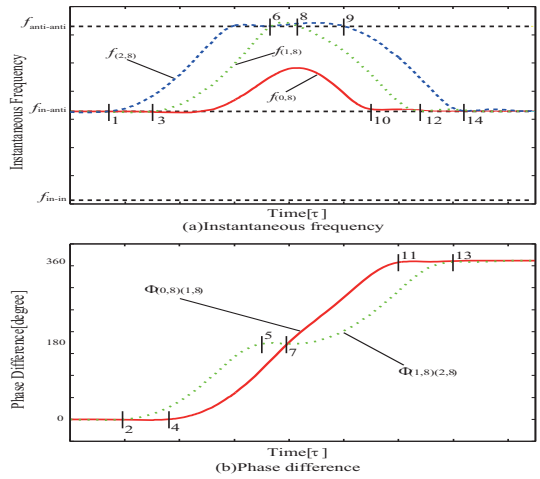

Figure 5: Transitions of phase differences and frequencies by reflecting a phase-inversion wave in in-and-anti-phase synchronous at an edge.

Table 2: Reflection of a phase-inversion wave at an edge in in-and-in-phase synchronous(see Fig.5).

no.	*Mechanism*
0	The phase state between adjacent oscillators of the horizontal direction is the anti-phase synchronous. A phase-inversion wave, which propagates from OSC(9,8) in anti-phase synchronous, arrives at OSC(2,8).
1	$f_{(2,8)}$ starts to increase from $f_{in-anti}$ toward $f_{anti-anti}$ by the phase-inversion wave.
2	$\Phi_{(1,8)(2,8)}$ starts to increase toward 180 degrees from 0, because $f_{(2,8)}$ increases toward $f_{anti-anti}$.
3	$f_{(1,8)}$ starts to increase from $f_{in-anti}$ toward $f_{anti-anti}$ because $\Phi_{(1,8)(2,8)}$ increases toward 180 degrees.
4	$\Phi_{(0,8)(1,8)}$ starts to increase toward 180 degrees from 0, because $f_{(1,8)}$ increases toward $f_{anti-anti}$.
5	$\Phi_{(1,8)(2,8)}$ arrives around 180 degrees, and it stabilizes the anti phase synchronous.
6	$f_{(1,8)}$ arrives $f_{anti-anti}$ because $\Phi_{(1,8)(2,8)}$ arrived 180 degrees.
7	$\Phi_{(0,8)(1,8)}$ is not steady in 180 degrees, and $\Phi_{(0,8)(1,8)}$ increases toward 360 degrees,because $f_{(1,8)}$ arrived at $f_{anti-anti}$. $f_{(0,8)}$ can not arrive at $f_{anti-anti}$. $f_{(0,8)}$ arrives middle $f_{anti-anti}$ and $f_{in-anti}$, and decrease to $f_{in-anti}$ again.
7.1	$\Phi_{(0,8)(1,8)}$ keeps passing 180 degrees, and it increasing toward 360 degrees.
8	$\Phi_{(0,8)(1,8)}$ does not stop 180 degrees, and $\Phi_{(0,8)(1,8)}$ continues to change to 360 degrees. Therefore, $f_{(1,8)}$ starts to decrease from $f_{anti-anti}$ to $f_{in-anti}$.
9	$f_{(2,8)}$ starts to decrease from $f_{anti-anti}$ toward $f_{in-anti}$ because $\Phi_{(1,8)(2,8)}$ increases toward 360 degrees from 180degrees.
10	$f_{(0,8)}$ arrives around $f_{in-anti}$.
11	$\Phi_{(0,8)(1,8)}$ arrives 360 degrees because $f_{(0,8)}$ arrived $f_{in-anti}$.
12	$f_{(1,8)}$ arrives $f_{in-anti}$ because $\Phi_{(0,8)(1,8)}$ arrived 360 degrees.
13	$\Phi_{(1,8)(2,8)}$ arrives 360 degrees because $f_{(1,8)}$ arrived $f_{in-anti}$.
14	$f_{(2,8)}$ arrives $f_{in-anti}$ because $\Phi_{(1,8)(2,8)}$ arrived 360 degrees.

4. Conclusion

We can observe reflecting phase-inversion waves at the edge in lattice oscillators. The reflections can be observed at the edge of lattice oscillators in in-and-in phase synchronous and in in-and-anti phase synchronous. These mechanisms of reflection phenomena were made clear by phase differences between adjacent oscillators and instantaneous frequencies of each oscillator.

At the corner of our system, a reflection of the phase-inversion wave can be observed. We should make clear the mechanism of the reflection.

Acknowledgements

This research is supported by the Grants-in-Aid for Young Scientific Research (B) (No. 19760270) from the Japan Society for the Promotion of Science.

References

[1] T. Endo and S. Mori, "Mode Analysis of Two-Dimensional Low-Pass Multimode Oscillator," *IEEE Trans. Circuits and Syst.*, vol. 23, no. 9, pp. 517-530, Sept. 1976.

[2] C. M. Gray, "Synchronous Oscillations in Neuronal Systems: Mechanisms and Functions," *Journal of Computational Neuroscience 1*, pp. 11–38, 1994.

[3] L. L. Bonilla, C. J. Pérez Vicente and R. Spigler, "Time-Periodic Phases in Populations of Nonlinearly Coupled Oscillators with Bimodal Frequency Distributions," *Physica D: Nonlinear Phenomena* vol. 113, issues 1, pp. 79–97, Feb. 1998.

[4] M. Yamauchi, Y. Nishio and A. Ushida, "Phase-Waves in a Ladder of Oscillators," *IEICE Trans. Fundamentals*, vol.E86-A, no.4, pp.891-899, Apr. 2003.

[5] M. Yamauchi, M. Okuda, Y. Nishio and A. Ushida, "Analysis of Phase-Inversion Waves in Coupled Oscillators Synchronizing at In-and-Anti-Phase," *IEICE Trans. Fundamentals*, vol.E86-A, no.7, pp.1799-1806, July 2003.

[6] S. Yamane, M. Yamauchi and Y. Nishio, "Classification of phenomena on coupled oscillators system as a lattice," *Proc. NCSP'09*, pp.249-252, Mar. 2009.

[7] T. Imoto, K. Ichiki, S. Yamane and M. Yamauchi, "Phase Difference Propagation Phenomena on a Non-edge Lattice," *Proc. NOLTA'08*, pp.616-619, Sept. 2008.